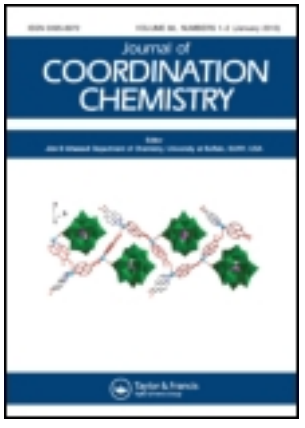

Journal of Coordination Chemistry
Publication details, including instructions for authors and subscription information:
http://www.tandfonline.com/loi/gcoo20

Metal-directed self-assembly of M_3L_2 (M=Zn, Cd) metal-organic architectures with a tripodal tris-bidentate chelator

Hai-Bin Zhu [a], Wen-Na Yang [a] & Jun Hu [b]

[a] School of Chemistry and Chemical Engineering, Southeast University, Nanjing, P.R. China

[b] Coordination Chemistry Institute, Nanjing University, Nanjing, P.R. China

Accepted author version posted online: 14 Jun 2013.Published online: 16 Jul 2013.

To cite this article: Hai-Bin Zhu, Wen-Na Yang & Jun Hu (2013) Metal-directed self-assembly of M_3L_2 (M=Zn, Cd) metal-organic architectures with a tripodal tris-bidentate chelator, Journal of Coordination Chemistry, 66:16, 2775-2787, DOI: 10.1080/00958972.2013.815344

To link to this article: http://dx.doi.org/10.1080/00958972.2013.815344

Journal of Coordination Chemistry, 2013
Vol. 66, No. 16, 2775–2787, http://dx.doi.org/10.1080/00958972.2013.815344

Metal-directed self-assembly of M_3L_2 (M=Zn, Cd) metal-organic architectures with a tripodal tris-bidentate chelator

HAI-BIN ZHU*†, WEN-NA YANG† and JUN HU‡

†School of Chemistry and Chemical Engineering, Southeast University, Nanjing, P.R. China

‡Coordination Chemistry Institute, Nanjing University, Nanjing, P.R. China

(*Received 18 December 2012; in final form 6 May 2013*)

Two discrete M_3L_2 metal-organic architectures, **1** and **2**, have been constructed by reaction of a newly designed tripodal tris-bidentate ligand **L** with $M(NO_3)_2$ (**1**: M=Zn; **2**: M=Cd). Both complexes together with **L** have been structurally elucidated by single-crystal X-ray crystallography. Complex **1** exhibits a cationic M_3L_2 coordination architecture bearing three positive charges balanced by three uncoordinated nitrates, while **2** shows a neutral M_3L_2. **1** and **2** both adopt a compressed trigonal prism shape but show no internal cavity due to close ligand-to-ligand interactions. They display totally different intermolecular packing modes in the solid state, which strongly influence the intermolecular π–π interactions. Complex **1** has been arrayed such that each M_3L_2 is surrounded by three neighboring C_3-symmetry related ones, whereas **2** exhibits a columnar molecular stacking. The distinctive intermolecular packing modes in the solid state between **1** and **2** bring about a small but discernible red shift (4 nm) corresponding to the π–π^* electronic absorption.

Keywords: Metal-organic polyhedra; Tripodal; Crystal structure; Photophysical property

1. Introduction

Metal-organic polyhedra (MOPs) are discrete metal-organic molecular assemblies, the synthetic approaches of which have been well explored such as symmetry interaction, molecular library, reticular chemistry, etc. [1–4], all based on spontaneous self-assembly of multiple (generally two) components in solution. Largely because of well-defined cavities with various functions, conventional MOPs serve as versatile hosts for molecular recognition [5, 6], gas separation and storage [7–9], catalysis [10–12], etc. [13–15]. More exciting developments in this area highlight the application of MOPs for nanoreactors [16–18] or drug delivery [19–22], and stabilizing reactive intermediates [23–25]. There is also interest in using MOPs as supramolecular building blocks (SBBs) in the construction of MOFs [26], which show advantages over the conventional secondary building unit approach given that some unique properties of MOPs might be directly transferred into those of the MOFs.

*Corresponding author. Email: zhuhaibin@seu.edu.cn

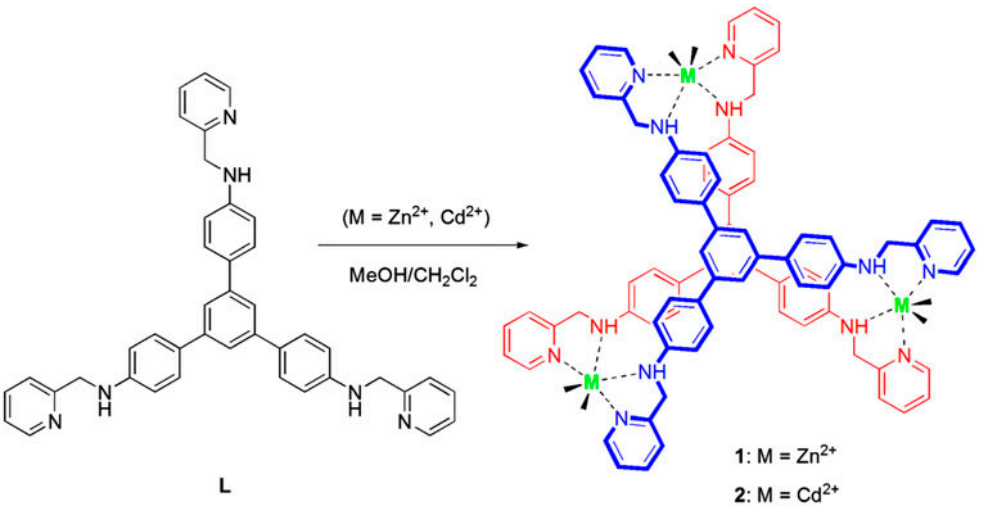

Chart 1. Compressed M_3L_2 metal-organic assemblies with **L**.

MOPs with M_3L_2 stoichiometry represent the simplest three-dimensional (3-D) closed supramolecular architecture, generally fabricated by coupling two tripodal ligands with three ditopic tectons [27–32]. In this contribution, we have prepared a tripodal tris-bidentate **L**, the reaction of which with $M(NO_3)_2$ led to two discrete M_3L_2 metal-organic assemblies (**1**: M=Zn; **2**: M=Cd) (chart 1). Compared to conventional M_3L_2 MOPs, they show considerably flattened structures with no cavity. Despite structural similarity, they exhibit totally different molecular packing modes in the solid state that impact intermolecular π–π interactions.

2. Experimental

2.1. *Materials and measurements*

All solvents and reagents of analytical grade and were used as received. The triamine **1** for **L** preparation was synthesized according to literature method [33]. Infrared spectra were recorded on a Thermo Scientific Nicolet 5700 FT-IR spectrophotometer with KBr pellets from 400–4000 cm^{-1}. ^1H NMR spectra were recorded with a Bruker AVANCE-500 spectrometer. Electrospray ionization (ESI) mass spectra were recorded on a Finnigan MAT SSQ 710 mass spectrometer in a scan range of 100–1200 amu. Powder X-ray diffraction (PXRD) data were recorded on a Siemens Bruker D5000 X-ray Powder Diffractometer. Solid state diffuse reflectance UV–vis spectra were obtained on a Shimadzu UV-2450 UV–vis spectrophotometer. Luminescence spectra for the solid samples were recorded at room temperature on a FluoroMax-4 spectrofluorometer.

2.2. *Synthesis*

2.2.1. Synthesis of L. To a solution of triamine **1** (3 g, 8.5 mM) in 200 mL of methanol was added 2-pyridinealdehyde (4.6 g, 43.0 mM) in one portion. The mixture was heated to

reflux and stirred for 6 h, $NaBH_4$ (3.2 g, 85.0 mM) was added in three portions into the reaction mixture which was pre-cooled in an ice bath, and then the reaction was further continued for 4 h under reflux. The reaction solution was poured into 200 mL of water and the resultant precipitate was collected by suction filtration. After thorough washing with water, the pale yellow solid was dried in vacuum for 24 h.

Yield: 4.9 g (87%). IR (KBr, cm^{-1}): ν 3403 m, 3022w, 1612s, 1592 m, 1569w, 1520s, 1473w, 1431 m, 1325w, 1294w, 1190w, 820 m, 756 m, 705w. ^{1}H-NMR ($CDCl_3$, 25 °C) $\delta = 8.69$ (d, 3H), 7.75–7.53 (m, 12H), 7.36 (m, 3H), 7.19 (m, 3H), 6.76 (m, 6H), 4.87 (br, 3H), 4.51 (s, 6H). ESI-MS (m/z,%) 625 (100%) $[\mathbf{L}+H^+]^+$; 647 (40%) $[\mathbf{L}+Na^+]^+$. Anal. $C_{42}H_{36}N_6$: Calcd C 80.74, H 5.81, N 13.45%; found C, 80.72, H 5.76, N 13.56%.

2.2.2. Preparation of 1 and 2. General procedure: At room temperature, a methanol solution (5 mL) of the metal salts (0.06 mM) (**1**: $Zn(NO_3)_2$; **2**: $Cd(NO_3)_2$) was carefully layered above dichloromethane solution (5 mL) of **L** (0.02 mM). A quantity of crystals was obtained over two weeks. Single crystal suitable for X-ray diffraction analysis was selected from the bulk crystals.

Complex **1**: Yield: 53% (based on **L**). IR (KBr, cm^{-1}): ν 3416 m, 3222 m, 3025w, 1608s, 1515s, 1478s, 1431 m, 1382s, 1204w, 1014w, 825 m, 764 m. ^{1}H-NMR (d_6-DMSO, 25 °C) $\delta = 8.54$ (d, 6H), 7.76 (t, 6H), 7.49 (t, 18H), 7.40 (d, 6H), 7.27 (t, 6H), 6.69 (d, 12H), 6.51 (br, 6H), 4.41 (s, 12H). Anal. $C_{168}H_{148}N_{36}O_{38}Zn_6$: Calcd C 54.95, H 4.06, N 13.73%; found C, 55.10, H 4.30, N 13.58%.

Complex **2**: Yield: 61% (based on **L**). IR (KBr, cm^{-1}): ν 3399 m, 3230 m, 3023w, 1606s, 1517s, 1433s, 1383s, 1311s, 1014w, 825 m, 765 m. ^{1}H-NMR (d_6-DMSO, 25 °C) $\delta = 8.54$ (d, 6H), 7.75 (t, 6H), 7.48 (t, 18H), 7.40 (d, 6H), 7.26 (t, 6H), 6.69 (d, 12H), 6.49 (br, 6H), 4.41 (s, 12H). Anal. $C_{168}H_{156}Cd_6N_{36}O_{42}$: Calcd C 50.12, H 3.91, N 12.53%; found C, 50.21, H 4.12, N 12.38%.

Table 1. Crystallographic data for **L**, **1** and **2**.

Compound	**L**	**1**	**2**
Formula	$C_{42}H_{36}N_6$	$C_{168}H_{148}N_{36}O_{38}Zn_6$	$C_{168}H_{156}Cd_6N_{36}O_{42}$
M_r	624.77	3671.44	4025.69
Crystal system	Triclinic	Cubic	Trigonal
Space group	*P*-1 (No. 2)	*I*a-3d (No. 230)	*P*-3*c*1 (No. 165)
a (Å)	5.9080(3)	31.740(1)	19.373(1)
b (Å)	12.4643(8)	31.740(1)	19.373(1)
c (Å)	24.088(2)	31.740(1)	13.875(1)
α (°)	99.745(5)	90	90
β	91.352(4)	90	90
γ	92.303(4)	90	120
V (Å^3)	1745.9(2)	31,976(3)	4510(1)
Z	2	8	1
D_{Calc} (g cm^{-3})	1.188	1.525	1.482
F (0 0 0)	660	15,136	2040
Reflns. collected	14,699	67,432	25,927
Unique reflns.	5472	2580	2966
R(int)	0.047	0.094	0.050
R_1, wR_2 [$I > 2\sigma(I)$]	0.0914/0.1735	0.0543/0.1292	0.0465/0.1179
R_1, wR_2 (all data)	0.1266/0.1836	0.0645/0.1356	0.0487/0.1220
GOF	1.01	1.09	1.04

2.3. *X-ray crystallography*

Diffraction intensity data for **L** were collected at 298(2) K on an Oxford Diffraction Xcalibur, Sapphire 3, Gemini ultra diffractometer employing enhanced ultra (Cu) X-ray source Cu–Kα radiation ($\lambda = 1.5418$ Å), and the diffraction intensity data for **1** and **2** were collected at 298(2) K on a Bruker SMART CCD-4K diffractometer employing graphite-monochromated Mo–Kα radiation ($\lambda = 0.71073$ Å). The data were collected using SMART and were reduced by SAINT [34]. The structures were solved by direct methods and refined by full-matrix least-squares on F^2_{obs} by using SHELXTL-PC software package [35]. All non-hydrogen atoms were refined anisotropically and all hydrogens were calculated and refined as a riding model. Graphics for **L**, **1** and **2** were generated using MERCURY 3.0 [36]. Crystallographic data for **L**, **1** and **2** are listed in table 1.

3. Results and discussion

3.1. *Synthesis and characterization of L*

Synthesis of **L** is outlined in scheme 1. Condensation of triamine **1** and 2-pyridinealdehyde in methanol resulted in the imine intermediate **2**, which was subsequently reduced by excess $NaBH_4$ to afford **L**. This procedure was carried out in a one-pot reaction without separating **2**. Analytically pure **L** can be easily obtained simply by filtration and water washing. The successful synthesis of **L** was verified by microanalytical characterizations, which agree well with its formula. In ^{1}H-NMR spectra, the signal at 4.51 ppm corresponds to the methylene protons and the signals corresponding to the aromatic protons are from 6.76 to 8.69 ppm. The positive ion ESI–MS spectrum of **L** displays two peaks at m/z 625 and 647, which correspond to its protonated ion $[\mathbf{L}+H^+]^+$ and sodium adduct $[\mathbf{L}+Na^+]^+$, respectively.

Diffraction-quality single crystals of **L** were grown by slow evaporation of its ethyl acetate/acetone solution. Single crystal X-ray diffraction offers more structural information of

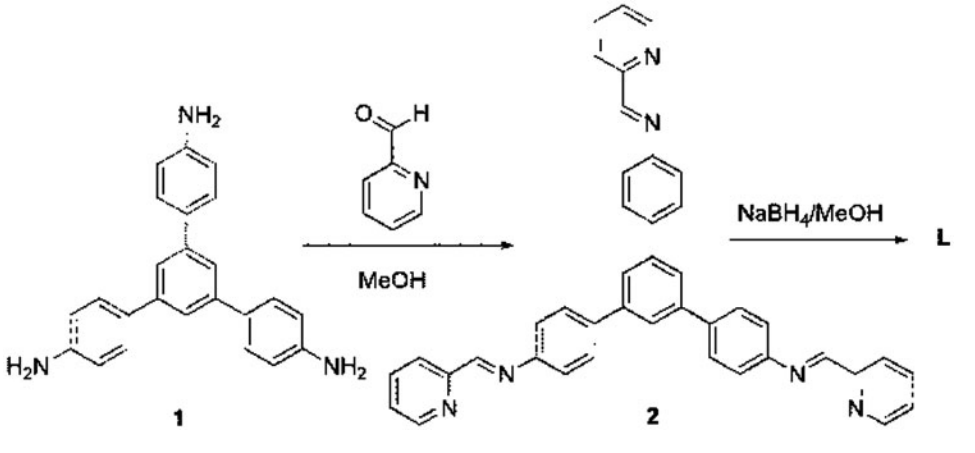

Scheme 1. Synthesis of **L**.

L in the solid state. As depicted in figure 1, **L** has triamine **1** as its central core equipped with three pyridine arms via C–N single bond. The three outer phenyl rings are not coplanar to the central one, forming three different dihedral angles (52.04°, 26.52°, and 30.57°). Among the outer phenyl rings, two have opposite rotational direction to the third with reference to the central phenyl ring. For the pyridine arms, two interact with the secondary amine through intramolecular N–H···N hydrogen bonds (N4···N3: 2.629(6) Å, N4–H4A···N3, 110°; N6···N5: 2.625(5) Å, N6-H6A···N5, 109°), which render the

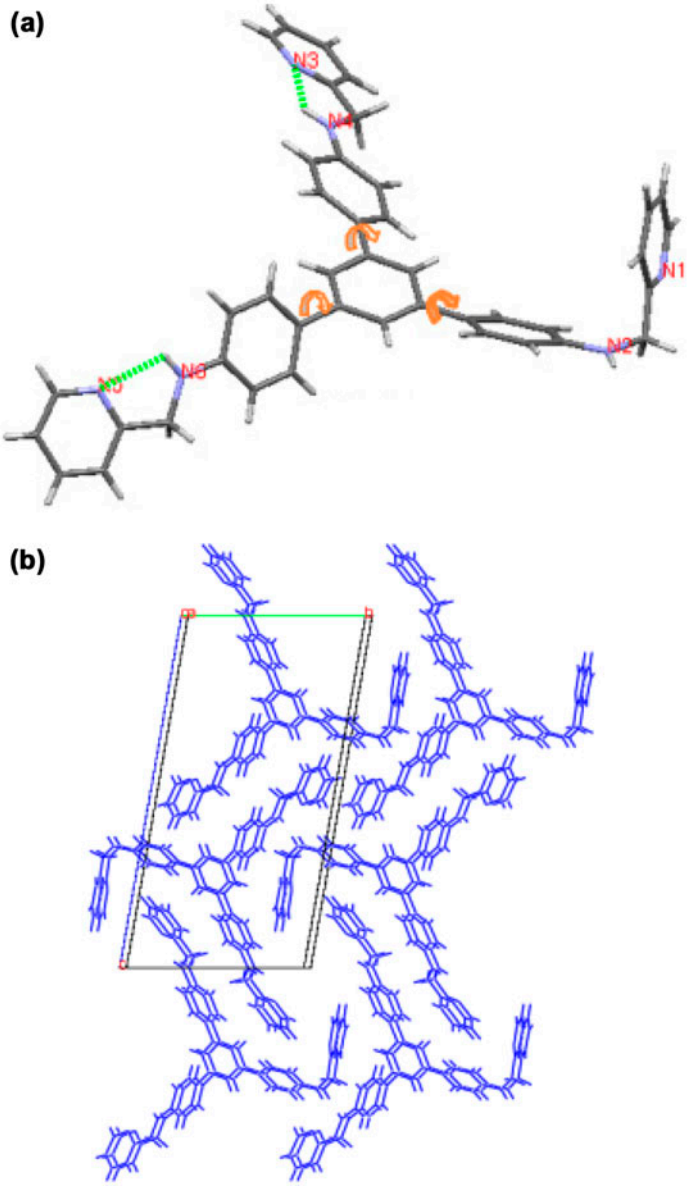

Figure 1. Crystal structure (a) and packing structure (b) of **L** (intramolecular hydrogen bonds and rotational directions denoted by the dotted line and arrows, respectively).

pyridine ring almost coplanar to its attached phenyl ring (dihedral angle: 8.8° and 10°). By contrast, the third makes a large dihedral angle of 80.9° with its linked phenyl ring due to lack of intramolecular hydrogen bonding interactions. On the basis of the above discussions, **L** actually loses its C_3-symmetry in the solid state. Appreciable aromatic π–π interactions do not exist except for extensive intermolecular C–H$\cdots\pi$ interactions observed in its packing structure (Supplementary material, table S1).

Raymond *et al.* reported a similar tripodal tris-bidentate chelator based on the same central triamine core but with coordinating catehol units attached to the central core via a relatively rigid amide linkage [37]. **L** has pyridine units linked to the central core through flexible C–N single bonds, which is expected to no longer follow the symmetry-driven rule proposed by Raymond for the construction of M_4L_4 tetrahedral coordination cages [38–40]. **L** resembles the reported imidazole-end capped tripodal ligand considering that they both possess a rigid central core and flexible linkages for coordinating arms [27, 28, 30, 31]. Self-assembly of the imidazole-based tripodal ligand with Ag(I), Cu(II), or Zn(II) prefers the M_2L_3 coordination cage that typically shows room for guest accommodation. However, possible M_2L_3 metal-organic architectures in this case should reduce their internal space because metal-coordination with the amine of **L** would pull two **L** significantly close. The close approach of two ligands can enhance ligand-to-ligand interactions, which may be of interest in some electrically conductive molecular materials [41–45].

3.2. *Preparation and characterization of 1 and 2*

Preparations of **1** and **2** were carried out at ambient temperature through a layering method, from which were obtained yellow block crystals. Single crystal X-ray diffraction analyses show that both adopt discrete M_3L_2 coordination architectures as anticipated. The phase purity of each complex is certified by comparing the simulated PXRD pattern with the experimental PXRD pattern (Supplementary material, figures S1 and S2). Complexes **1** and **2** are insoluble in EtOH, MeOH, and H_2O but readily dissolve in DMSO. ^{1}H-NMR characterizations in d_6-DMSO reveal that both complexes have similar resonances as those for free **L** in terms of the aromatic and methylene protons. The only difference is found for the amine proton signal which turns broad in **1** and **2** compared to free **L** (Supplementary material, figure S3). The amine proton signal broadening, we speculated, is caused by metal coordination, which renders the amine proton more reactive and facilitates the exchange with water. Unfortunately, ESI–MS characterizations of **1** and **2** failed to detect m/z peaks which could be reasonably assigned to the M_3L_2 species. On the contrary, free **L** as $[\mathbf{L}+H^+]^+$ at m/z 625 is clearly observed. Accordingly, it suggests that **1** and **2** cannot remain intact under ESI–MS conditions, under which metal–ligand dissociation should occur.

3.3. *Structure description of 1 and 2*

Complex **1** crystallizes in the cubic crystal system and *I*a-3d space group. As shown in figure 2, **1** exhibits a discrete M_3L_2 coordination architecture which constitutes two **L**, three Zn^{2+}, and three nitrates. Thereby, **1** bears three positive charges balanced by three uncoordinated nitrates. Unlike free **L**, each **L** in **1** is a C_3-symmetric tripodal tris-bidentate chelator of which three outer phenyl rings have the same rotational direction with respect to the central one, forming a dihedral angle of 39.5(3)°. The three pyridines adopt identical conformations, each having a dihedral angle of 77.0(2)° with its attached phenyl ring. In

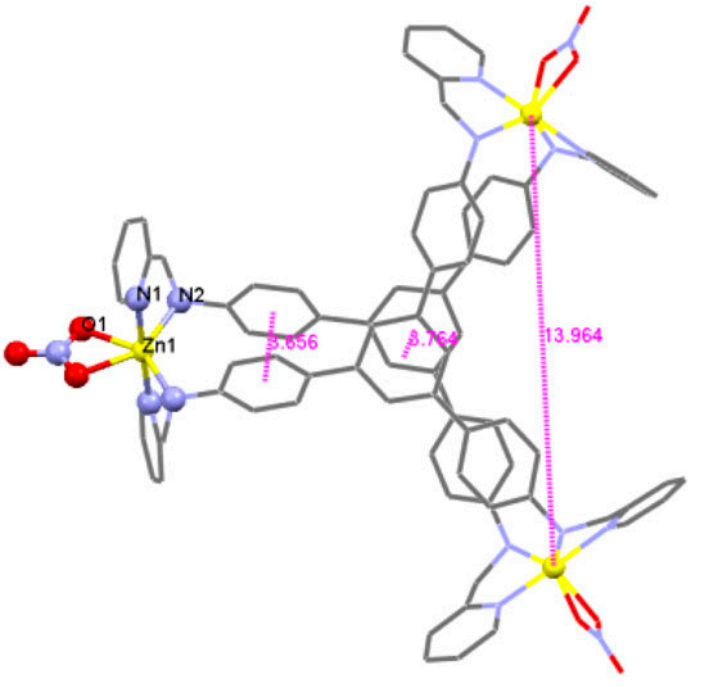

Figure 2. Crystal structure of **1** (hydrogens, uncoordinated nitrate, and solvent omitted for clarity).

1, each six-coordinate Zn^{2+} is bound by two sets of NN-chelating donors from two **L** and two oxygens from one nitrate. The Zn–N distance (2.170(2) Å) between Zn^{2+} and N from the secondary amine is a little longer than that (2.065(3) Å) for pyridine. Each bound nitrate occupies two coordination sites of one Zn^{2+} in a O–N–O chelating mode with a Zn–O distance of 2.225(2) Å and a O–Zn–O bite angle of 60.0(1)°. Taking a close look at the geometric parameters around Zn^{2+} (Supplementary material, table S2), the coordination geometry of the Zn^{2+} ion is better described as a distorted octahedron with two pyridine N occupying the axial sites. Metal coordination of the secondary amine in **L** forces two **L** ligands in close proximity in **1**, which is evidenced by the short ligand-to-ligand separation. Two central phenyl rings from two **L** in the same M_3L_2 molecule are strictly parallel, adopting a face to face orientation with a centroid to centroid distance of 3.764 Å. However, each outer phenyl ring from one **L** is tilted by a small dihedral angle of 5.86° and with a separation of 3.656 Å. Moreover, three Zn^{2+} ions are symmetrically disposed about a molecular C_3 axis with a Zn···Zn separation of 13.964 Å. Compared to reported M_3L_2 MOPs [27–32], **1** looks like a compressed trigonal prism but has no cavity to accommodate guest molecules.

In the packing structure of **1** (figure 3), each M_3L_2 unit (pink) is surrounded by three other ones (blue) which are symmetrically distributed around a threefold axis. Specifically, each plane defined by three Zn^{2+} ions in the outer M_3L_2 unit leans against that in the central one by a dihedral angle of 70.5°. Obviously, such molecular arrangement in **1** discourages close intermolecular stacking interactions, and indeed the supramolecular interactions in the packing structure are mainly involved with C–H···π and N–O···π interactions (Supplementary material, table S1).

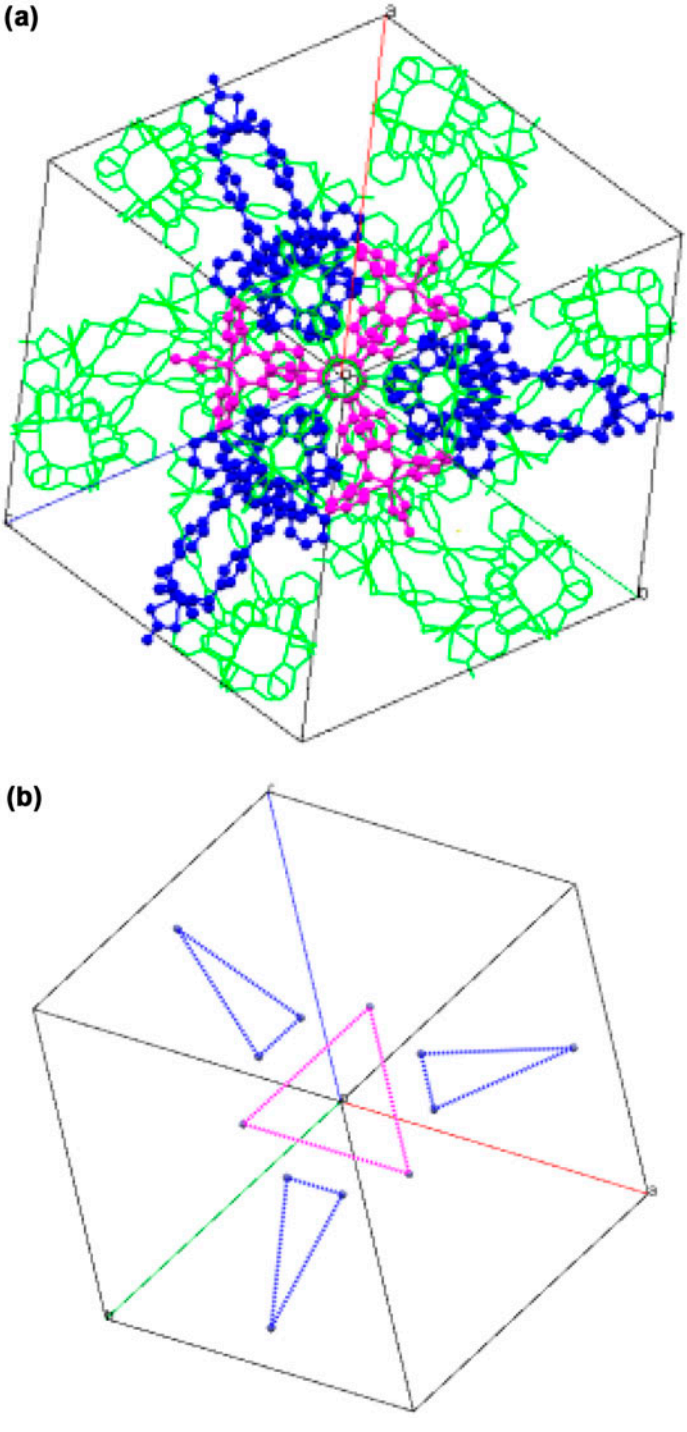

Figure 3. (a) Intermolecular arrangement in **1** in the unit cell; (b) space orientation of the planes defined by three Zn^{2+} ions in M_3L_2.

Complex **2** crystallizes in the trigonal crystal system and *P*-3*c*1 space group. Similar to **1**, **2** also has a M_3L_2 coordination architecture, comprised of two **L**, three Cd^{2+} ions, and six nitrates (figure 4). As a result, **2** is neutral, different from the cationic **1**. Likewise, **L** in **2** also is a C_3-symmetric tripodal tris-bidentate chelator with geometric parameters comparable to that in **1**. Each Cd^{2+} is six-coordinate by two sets of NN-chelating donors from two **L** and two oxygens from two nitrates. Similarly, the Cd–N(amine) bond (2.440(2) Å) is slightly longer than the Cd–N(pyridine) bond (2.336(2) Å). Unlike **1**, each nitrate in **2** has unidentate coordination with a Cd–O bond distance of 2.363(2) Å. Taking the geometric data around Cd^{2+} together (Supplementary material, table S2), each Cd^{2+} in **2** is better delineated as a distorted trigonal prism. In **2**, two parallel central phenyl rings from two **L** overlay each other with a shorter separation (centroid to centroid distance: 3.553 Å; slippage: 0). Strikingly, each outer phenyl ring from one **L** is also parallel to the respective one from another with a separation of 3.703 Å (slippage: 1.342 Å). The intermetallic Cd···Cd distance in **2** is 14.502 Å. Compared to **1**, **2** seems more compressed, which eliminates any possibility for guest inclusion.

Complex **2** in its solid state exhibits a columnar stacking fashion in terms of intermolecular arrangement. As shown in figure 5, there are two types of M_3L_2 units, A and B, alternately with one related to the next by a 60° rotation around a common threefold axis. The rotational direction of propeller-like **L** in A and B is right opposite. There exist close intermolecular aromatic π–π interactions between central phenyl rings from neighboring M_3L_2 units, as indicated by the centroid to centroid separation of 3.384 Å, similar to the value in graphite (3.35 Å). Such molecular arrangement in **2** leads to the creation of beautiful snowflake-like patterns along the *ab* plane.

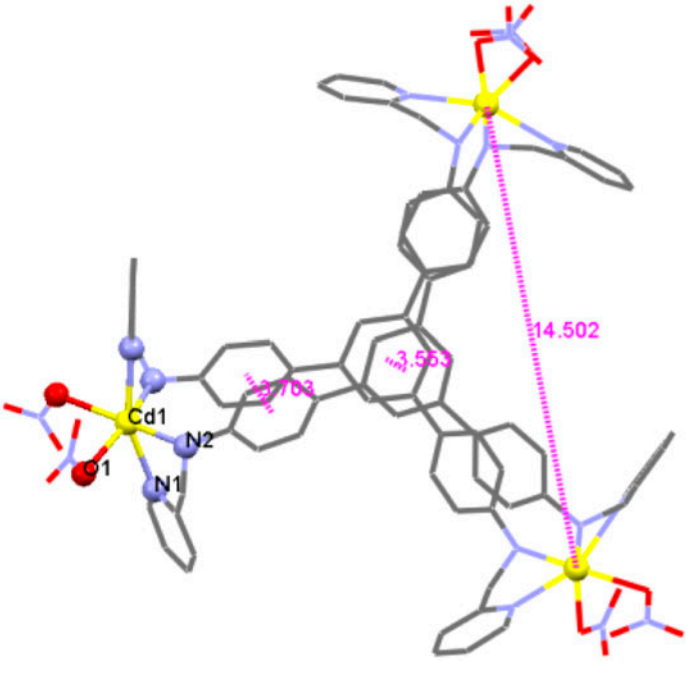

Figure 4. Crystal structure of **2** (hydrogens and solvent molecules omitted for clarity).

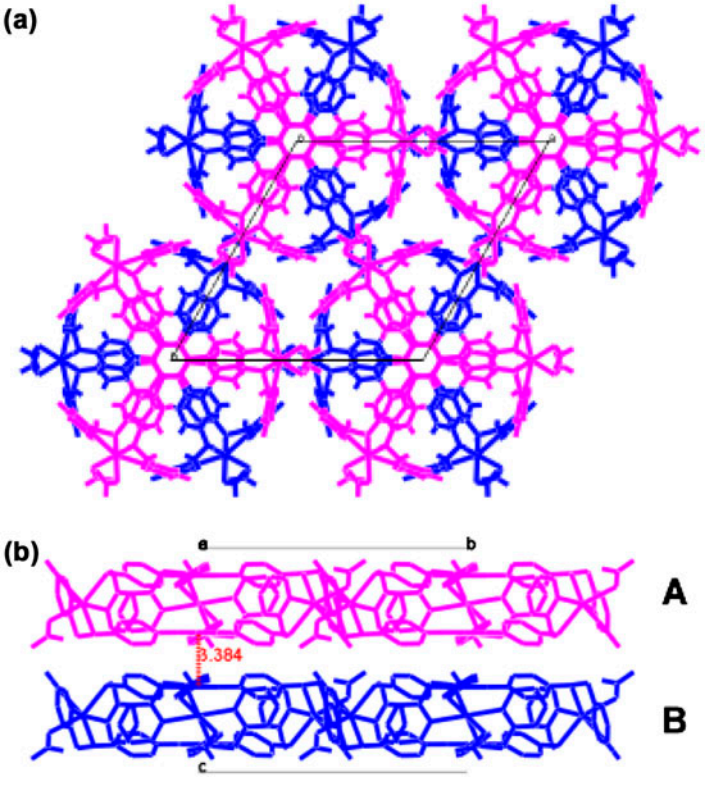

Figure 5. Intermolecular arrangement in **2** (a) top view; (b) side view.

Compared to the conventional M_3L_2 MOPs, **1** and **2** display a rare compressed trigonal prism-like shape without any cavity, which is very close to the flattened trigonal bipyramidal complex $[Pd_3(L1)_2(O_2CCH_3)_6]$ (L1 = N,N′,N″-tris(6-methyl-2-pyridyl)benzene-1,3,5-tricarboxamide) [46]. Furthermore, **1** and **2** both feature a discrete triangular trinuclear motif (for **1**, Zn_3; for **2**, Cd_3), which are separated by two C_3-symmetric **L**. It is distinguished from trinuclear zinc or cadmium units in the literature, which exist as metals bridged by carboxylate O or Cl, etc. and serve as inorganic nodes in coordination polymers [47–50]. Each metal ion in **1** and **2** is coordinated by one or two nitrates, which can be further substituted by other organic bridges such as 4,4′-bypridine. In this regard, discrete **1** and **2** might work as SBBs for the construction of MOP-based MOFs, which are currently underway in our laboratory.

3.4. *Photophysical properties of 1 and 2*

As discussed above, **1** and **2** in the solid state have different molecule organizations. In **2**, columnar molecule stacking allows for effective aromatic π–π interactions. The molecule arrangement in **1** would markedly diminish such interaction. We assumed that the photophysical properties of **1** and **2** may be sensitive to change in aromatic π–π interactions. Therefore, solid state diffuse reflectance UV–vis spectroscopy was performed on crystal samples of **1** and **2**. As depicted in figure 6, both the complexes show two absorptions

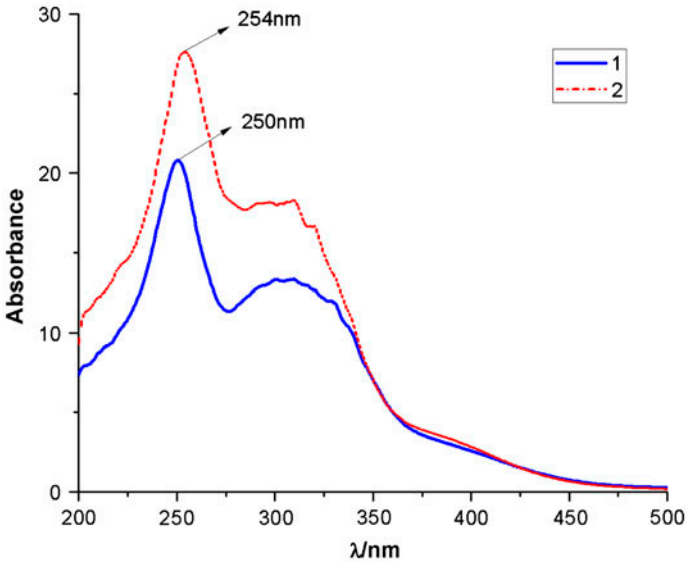

Figure 6. Diffuse reflectance UV–vis spectra of **1** and **2**.

from 200 to 500 nm. One at ca. 250 nm originated from π–π^* transition, the other at 305 nm is assigned to n–π^* transition. For the π–π^* transition, **2** exhibits a small but discernible red shift in absorption wavelength in comparison to **1** (**1**: 250 nm; **2**: 254 nm), which is in accord with its more effective intermolecular aromatic π–π interactions. The photoluminescent properties of **1** and **2** were also examined in solid state at ambient temperature. **L** displays luminescence with maxima at 410 nm and 510 nm upon excitation at 300 nm. However, no clear luminescence properties are observed for **1** and **2** suggesting that luminescence of **L** is quenched by metal coordination.

4. Conclusion

Self-assembly of tripodal tris-bidentate chelator **L** with $M(NO_3)_2$ led to two M_3L_2 coordination architectures, **1** and **2** (**1**: M=Zn; **2**: M=Cd), with similar size and shape. The metal coordination of amine of **L** results in remarkable reduction in their internal space such that they have no cavity to enclose a guest molecule. Complex **2** exhibits an interesting columnar stacking with respect to intermolecular arrangement, which permit close aromatic π–π interactions. It is assumed that the neutral nature of **2** may favor such columnar stacking, since it should have less Coulombic repulsions than the cationic **1**. Such columnar intermolecular stacking in **2** has an impact on its photophysical properties in solid state as a result of effective intermolecular aromatic π–π interactions.

Supplementary material

CCDC-908644 (for **1**), -908645 (for **2**) and -908646 (for **L**) contain the supplementary crystallographic data for this paper. These data can be obtained free of charge via http://

www.ccdc.cam.ac.uk/conts/retrieving.html, or from the Cambridge Crystallographic Data Centre, CCDC, 12 Union Road, Cambridge CB2 1EZ, UK (Fax: 44-1223-336-033; or E-mail: deposit@ccdc.cam.ac.uk).

Acknowledgments

We acknowledge the financial support from the National Natural Science Foundation of China (No. 21171036) and the Teaching and Research Program for the Excellent Young Teachers of Southeast University.

References

[1] D.L. Caulder, K.N. Raymondn. *Acc. Chem. Res.*, **32**, 975 (1999).
[2] S. Leininger, B. Olenyuk, P.J. Stang. *Chem. Rev.*, **100**, 853 (2000).
[3] M. Fujita, K. Umemoto, M. Yoshizawa, N. Fujita, T. Kusukawa, K. Biradha. *Chem. Commun.*, 509 (2001).
[4] D.J. Tranchemontagne, Z. Ni, M. O'Keeffe, O.M. Yaghi. *Angew. Chem. Int. Ed.*, **47**, 5136 (2008).
[5] K. Yamashita, M. Kawano, M. Fujita. *Chem. Commun.*, **4102**, (2007).
[6] C.R.K. Glasson, J.K. Clegg, J.C. McMurtrie, G.V. Meehan, L.F. Lindoy, C.A. Motti, B. Moubaraki, K.S. Murray, J.D. Cashion. *Chem. Sci.*, **2**, 540 (2011).
[7] J.R. Li, H.C. Zhou. *Angew. Chem. Int. Ed.*, **48**, 8465 (2009).
[8] Z. Lu, C.B. Knobler, H. Furukawa, B. Wang, G. Liu, O.M. Yaghi. *J. Am. Chem. Soc.*, **131**, 12532 (2009).
[9] D. Zhao, D.Q. Yuan, R. Krishna, J.M. Van Baten, H.C. Zhou. *Chem. Commun.*, **46**, 7352 (2010).
[10] W.G. Lu, D.Q. Yuan, A. Yakovenko, H.C. Zhou. *Chem. Commun.*, **47**, 4968 (2011).
[11] Z.J. Wang, C.J. Brown, R.G. Bergman, K.N. Raymond, F.D. Toste. *J. Am. Chem. Soc.*, **133**, 7358 (2011).
[12] M.M.J. Smulders, J.R. Nitschke. *Chem. Sci.*, **3**, 785 (2012).
[13] M. Yoshizawa, K. Ono, K. Kumazawa, T. Kato, M. Fujita. *J. Am. Chem. Soc.*, **127**, 10800 (2005).
[14] T. Osuga, T. Murase, K. Ono, Y. Yamauchi, M. Fujita. *J. Am. Chem. Soc.*, **132**, 15553 (2010).
[15] V. Vajpayee, Y.J. Yang, S.C. Kang, H. Kim, I.S. Kim, M. Wang, P.J. Stang, K.W. Chi. *Chem. Commun.*, **47**, 5184 (2011).
[16] T.S. Koblenz, J. Wassenaar, J.N.H. Reek. *Chem. Soc. Rev.*, **37**, 247 (2008).
[17] M.D. Pluth, R.G. Bergman, K.N. Raymond. *Acc. Chem. Res.*, **42**, 1650 (2009).
[18] M. Yoshizawa, J.K. Klosterman, M. Fujita. *Angew. Chem. Int. Ed.*, **48**, 3418 (2009).
[19] B. Therrien, G. Süss-Fink, P. Govindaswamy, A.K. Renfrew, P.J. Dyson. *Angew. Chem. Int. Ed.*, **47**, 3773 (2008).
[20] O. Zava, J. Mattsson, B. Therrien, P.J. Dyson. *Chem. Eur. J.*, **16**, 1428 (2010).
[21] D. Zhao, S.W. Tan, D.Q. Yuan, W.G. Lu, Y.H. Rezenom, H.L. Jiang, L.Q. Wang, H.C. Zhou. *Adv. Mater.*, **23**, 90 (2011).
[22] J.E.M. Lewis, E.L. Gavey, S.A. Cameron, J.D. Crowley. *Chem. Sci.*, **3**, 778 (2012).
[23] M. Yoshizawa, T. Kusukawa, M. Fujita, S. Sakamoto, K. Yamaguchi. *J. Am. Chem. Soc.*, **123**, 10455 (2001).
[24] M. Kawano, Y. Kobayashi, T. Ozeki, M. Fujita. *J. Am. Chem. Soc.*, **128**, 6558 (2006).
[25] P. Mal, B. Breiner, K. Rissanen, J.R. Nitschke. *Science*, **324**, 1697 (2009).
[26] M.J. Prakash, M.S. Lah. *Chem. Commun.*, **3326**, (2009).
[27] H.K. Liu, W.Y. Sun, D.J. Ma, K.B. Yu, W.X. Tang. *Chem. Commun.*, 591 (2000).
[28] W.Y. Sun, J. Fan, T. Okamura, J. Xie, K.B. Yu, N. Ueyama. *Chem. Eur. J.*, **7**, 2557 (2001).
[29] U. Radhakrishnan, M. Schweiger, P.J. Stang. *Org. Lett.*, **3**, 3141 (2001).
[30] J. Fan, W.Y. Sun, T. Okamura, J. Xie, W.X. Tang, N. Ueyama. *New J. Chem.*, **26**, 199 (2002).
[31] J. Fan, H.F. Zhu, T. Okamura, W.Y. Sun, W.X. Tang, N. Ueyama. *Chem. Eur. J.*, **9**, 4724 (2003).
[32] S. Mirtschinm, A. Slabon-Turski, R. Scopelliti, A.H. Velders, K. Severin. *J. Am. Chem. Soc.*, **132**, 14004 (2012).
[33] C. Bao, R. Lu, M. Jin, P. Xue, C. Tan, T. Xu, G. Liu, Y. Zhao. *Chem. Eur. J.*, **12**, 3287 (2006).
[34] Siemens. *SAINT Version 4 software Reference Manual*, Siemens Analytical X-ray Systems, Inc., Madison, Wiskonsin, USA (1996).
[35] Siemens. *SHELXTL, Version 5, Reference Manual,* Siemens Analytical X-ray Systems, Inc., Madison, Wiskonsin, USA (1996)
[36] C.F. Macrae, P.R. Edgington, P. McCabe, E. Pidcock, G.P. Shields, R. Taylor, M. Towler, J. van de Streek. *J. Appl. Cryst.*, **39**, 453 (2006).
[37] R.M. Yeh, J. Xu, G. Seeber, K.N. Raymond. *Inorg. Chem.*, **44**, 6228 (2005).
[38] C. Brückner, R.E. Powers, K.N. Raymond. *Angew. Chem. Int. Ed.*, **37**, 1837 (1998).

[39] D.L. Caulder, C. Brückner, R.E. Powers, S. König, T.N. Parac, J.A. Leary, K.N. Raymond. *J. Am. Chem. Soc.*, **123**, 8923 (2001).
[40] R.W. Saalfrank, H. Glaser, B. Demleitner, F. Hampel, M.M. Chowdhry, V. Schnemann, A.X. Trautwein, G.B.M. Vaughan, R. Yeh, A.V. Davis, K.N. Raymond. *Chem. Eur. J.*, **8**, 493 (2002).
[41] A. Aumüller, P. Erk, G. Klebe, S. Hünig, J.U. von Schütz, H.P. Werner. *Angew. Chem. Int. Ed. Engl.*, **25**, 740 (1986).
[42] A. Kobayashi, E. Fujiwara, H. Kobayashi. *Chem. Rev.*, **104**, 5243 (2004).
[43] Z. Coord. *Chem. Rev.*, **250**, 2745 (2006).
[44] M. Tadokoro, S. Yasuzuka, M. Nakamura, T. Shinoda, T. Tatenuma, M. Mitsumi, Y. Ozawa, K. Toriumi, H. Yoshino, D. Shiomi, K. Sata, T. Takui, T. Mori, K. Murata. *Angew. Chem. Int. Ed.*, **45**, 5144 (2006).
[45] G. Givaja, P. Amo-Ochoa, C.J. Gómez-García, F. Zamora. *Chem. Soc. Rev.*, **41**, 115 (2012).
[46] A. Westcott, J. Fisher, L.P. Harding, M.J. Hardie. *CrystEngComm*, **10**, 276 (2008).
[47] Q.-G. Zhai, R. Ding, S.-N. Li, Y.-C. Jiang, M.-C. Hu. *J. Coord. Chem.*, **65**, 516 (2012).
[48] L.-N. Yang, Y.-X. Zhi, J.-H. Hei, J. Li, F.-X. Zhang, S.-Y. Gao. *J. Coord. Chem.*, **64**, 2912 (2011).
[49] J.-S. Hu, Y.-J. Shang, X.-Q. Yao, L. Qin, Y.-Z. Li, Z.-J. Guo, H.-G. Zheng, Z.-L. Xue. *Cryst. Growth Des.*, **10**, 4135 (2010).
[50] G. Zhang, S. Wang, Q. Gan, Y. Zhang, G. Yang, J.S. Ma, H. Eur. *J. Inorg. Chem.*, 4186 (2005).